Eco-friendly AlON Processing

NKFI NNE 129976

-Final report -

The current research focus was oriented to the novel eco-friendly, comparatively low temperature fabrication of AlN-Al_2O_3 composite ceramics using the two-step oxidation and hot isostatic pressing technology (HIP). The aim of the investigations was to produce the AlN-Al_2O_3 composite in an environment friendly method. The current method has the advantages of lower processing temperature, time and energy requirements. The qualitative analysis of the obtained ceramic phase was analyzed by electron microscopy (SEM) and X-ray diffraction (XRD) techniques to observe the phase, composition and microstructure of the final AlN-Al_2O_3 composite. The samples were also tested for their mechanical and tribological properties.

The aim of this project in this term was to present a novel, a lower sintering temperature preparation, processing, structural, mechanical and tribological testing of the AlN-Al_2O_3 ceramics. The precursor powder of AlN was subjected to oxidation in ambient environment at 900 °C for 3, 10 and 20 hours, respectively (Fig. 1). The percentage of conversion between AlN and Al_2O_3 compounds depended on the time of oxidation as presented in Fig. 2.

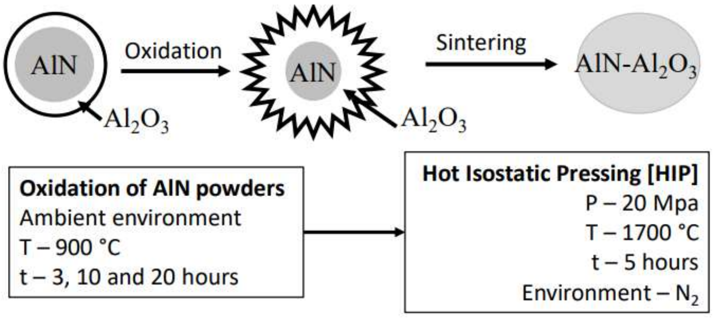

Oxidation of AlN powders
Ambient environment
T – 900 °C
t – 3, 10 and 20 hours

Hot Isostatic Pressing [HIP]
P – 20 Mpa
T – 1700 °C
t – 5 hours
Environment – N_2

Fig. 1. The schematic of oxidation of AlN powder and corresponding sintering process along with the parameters of processing.

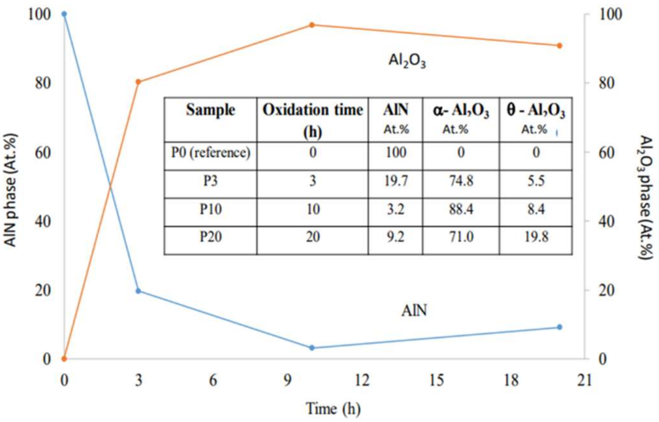

Sample	Oxidation time (h)	AlN At.%	α- Al_2O_3 At.%	θ - Al_2O_3 At.%
P0 (reference)	0	100	0	0
P3	3	19.7	74.8	5.5
P10	10	3.2	88.4	8.4
P20	20	9.2	71.0	19.8

Fig. 2. The change and phase transformation observed in the AlN and α-Al_2O_3 phases as function of oxidation time as shown in the table in the inset.

These oxidized powders were characterized by SEM and XRD to reveal their morphology, phase and crystal structure. The SEM results showed coarse powder particles and the presence of aluminum oxide (Al_2O_3) phase at the surface of aluminum nitride (AlN). The powders exhibited increasing oxidation and transition from AlN to Al_2O_3 phase. The oxidized AlN powder to AlN-Al_2O_3 was observed from SEM micrographs in Figure 3a–d after 0, 3, 10, and 20 hours respectively. It is visible that the powders consist of small, irregular shaped particles in the size of several hundred nanometers. The size distribution of particles is homogeneous in the case of reference AlN powder (Fig. 3a), however, after 3 and 6 hours of oxidation, some agglomerations are also appearing (Fig. 3b,c), the particles tended to cohere into larger blocks in micrometer size. The sample after 10 hours of oxidation shows very different morphology, in this case the size of the particles varies in wider dimensions. In addition, long, rod-like particles can also be found, indicating the phase transformation to be near complete. The increased oxidation time provides more time for the AlN powder to transform, leading to formation of aluminum oxide. Over the course of oxidized time, the powders exhibit growth of the dual phase AlN-Al_2O_3 composite.

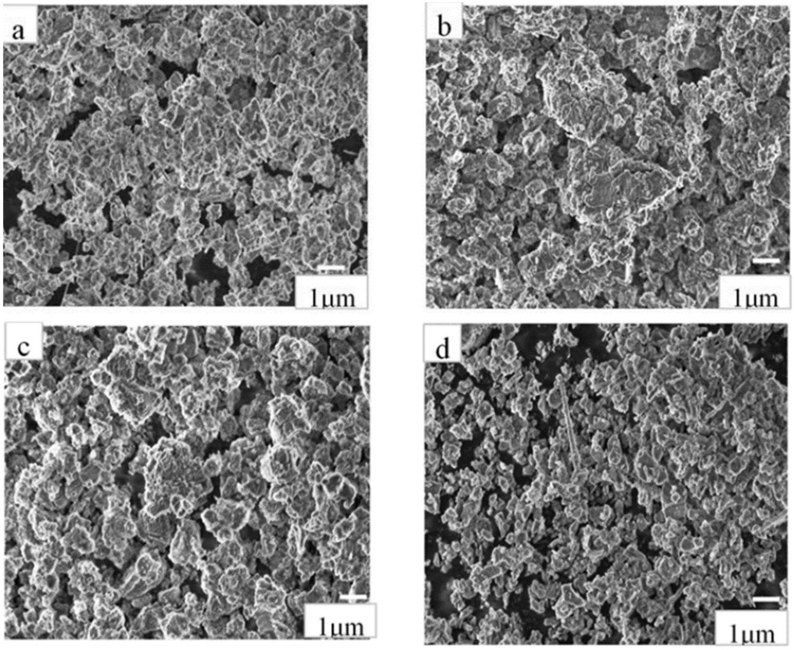

Fig. 3. Scanning electron micrographs of the oxidized microstructures of a) AlN, b-d) AlN powders oxidized for 3, 10 and 20 hours.

The XRD analysis has shown increasing aluminum-oxy-nitride conversion of aluminum nitride as the holding time of oxidation increased. The highest percentage of conversion of AlN powder to AlN-Al_2O_3 was observed after 10 hours. Simultaneously the powders were compacted and sintered using the hot isostatic pressing (HIP) under inert environment (N_2 gas) at 1700 °C, 20 MPa for 5 hours. This lead to the compaction and increase in density of the final samples.

Fig. 4 demonstrates the characteristic X-ray diffraction patterns of powders. It was confirmed that two different phases of aluminum oxide were grown simultaneously, α-Al_2O_3 (Rhombohedral, JCP2:00–010-0173) and the intermediary θ-Al_2O_3 (Monoclinic, JCP2:01-086-1410) upon oxidation of pure AlN (Hexagonal, JCP2:03-065-1902). Although the second phase of aluminum oxide can be observed only in the powders after 10 and 20 h of oxidation time. Since aluminum and aluminum nitride readily react with oxygen, the probability of transformation of AlN to Al_2O_3 is high. Some research works revealed that the intermediary phase has about 35.7 at% AlN and 64.3 at% Al_2O_3 at equilibrium [1]. Though XRD analysis shows formation of two phases of aluminum oxide, the dominant phase is α-Al_2O_3. In our XRD diffractograms of the oxidized powders, the signal pertaining to θ-Al_2O_3 at 30◦ , 36◦ , and 44◦ of 2θ position can only be seen in the oxidized powders at 10 and 20 hours oxidation time. The intermediary aluminum oxide phase, θ-Al_2O_3 was reported in other studies [2-5], which is in agreement with our results. The most commonly agreed fact is that AlN is mostly oxidation-resistant at temperatures below 850 ◦C. The initial oxidation of AlN exhibits a linear behavior and proceeds by formation of discontinuous and thin protective oxide film at the surface. This thin film is mostly porous and hence acts as a further oxidation site [2]. As the temperature increase above 950 ◦C, the AlN surface becomes more susceptible to oxidation. Above 1000 ◦C, the oxidation of the surface occurs abruptly and a thick film begins to form at the surface. Above 1050 ◦C, the oxidation follows a parabolic trend [3-5]. In our experiments, at 900 ◦C, α-Al_2O_3 was formed exhibiting a coarse structure on the surface (Fig. 3). Generally, α-Al_2O_3 is a thermodynamically stable structure of the aluminum oxide phases with a rhombohedral crystal structure. Other structures of alumina include monoclinic θ-Al_2O_3 and tetragonal δ-Al_2O_3 which are usually transition phases of alumina as investigated by Duchesne and Hipps [6] and Gu nd Edgar [7]. The presence of θ-Al_2O_3 is proof of the formation of transition alumina and hence the intermediary oxynitride generation in the powders.

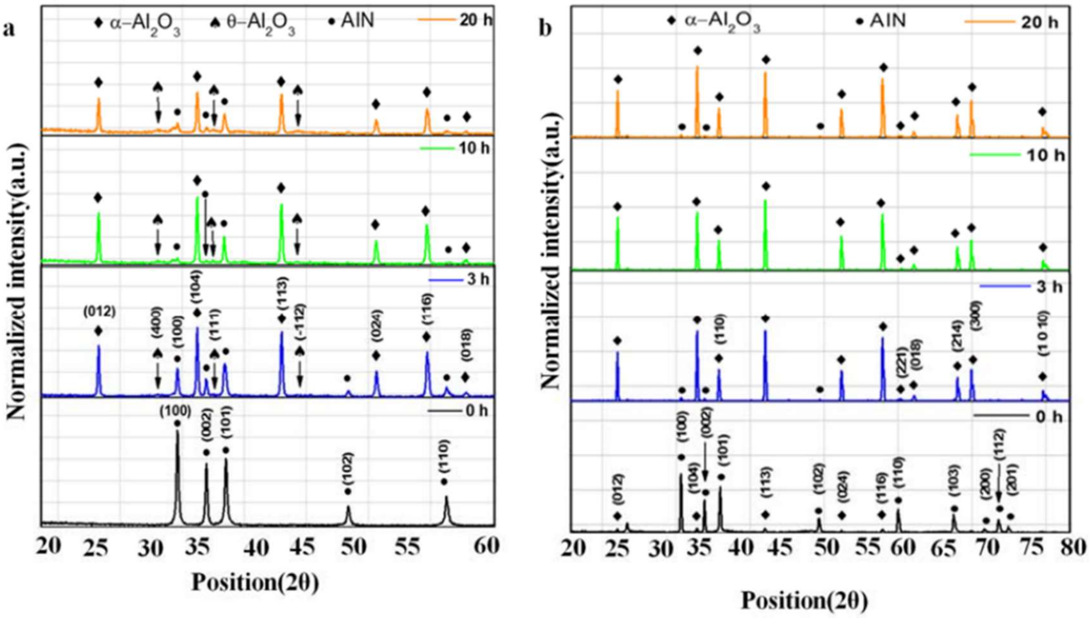

Fig. 4. XRD diffractograms of both oxidized powders (a) and sintered samples (b). Oxidation has resulted in the conversion of pure AlN (at 0 h) to two distinct phases of aluminum oxide namely α-Al_2O_3 and θ-Al_2O_3 (at 3, 10, and 20 h) in (a). The sintered samples on the other hand show presence of only α-Al_2O_3 besides AlN, proving that the sintering results in disintegration of θ-Al_2O_3 phase.

Mechanical tests, such as bending test and tribology tests were carried out on the samples. The mechanical properties of the samples were observed to improve in the oxidized samples compared to the precursor AlN. Moreover, applying longer oxidation time, the mechanical properties of the sintered samples enhanced significantly. Optimum qualitative (microstructure, oxide percentage) and quantitative (tribology, hardness and bending tests) properties were observed in samples with 0, 3, 10 and 20 hours oxidation time.

The sintered composites were tested for their mechanical properties such as microhardness test and bending tests to quantify their mechanical strength and hardness. Both three-point and four-point bending tests conducted on the sintered oxidized composites showed an increase in the bending strength of the samples compared to the non-oxidized samples. Similar trend in results was observed in hardness test. Both sets of values increased as function of oxidation time initially provided for the AlN powders and the plots can be seen in Fig. 5. The bending strength of the sintered samples according to the 3-point bending test was ~25 MPa (for AlN, non-oxidized sample) and 204 MPa (sintered after 10 hours oxidation). The values for 4-point bending tests were ~14 MPa (for AlN, non-oxidized sample) and 154 MPa (sintered after 10 hours oxidation, see Fig. 5a).

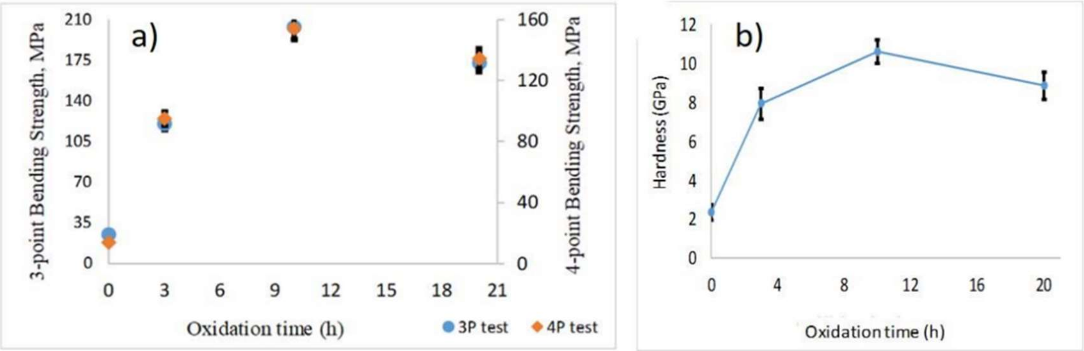

Fig. 5 The measured 3-point and 4-point bending strength (a) and micro-hardness (b) of the sintered AlN-Al_2O_3 given as function of oxidizing time of the samples.

The generally observed trend of improved mechanical properties of the sintered AlN-Al_2O_3 samples were attributed to the refinement in the microstructure as reported by Swab et al. and others [8-10]. A similar effect has been observed in our case as the transformation of AlN to Al_2O_3 has imparted strength to the sintered composite. HIP sintering helps in the dispersion of the Al_2O_3 phase across the surface of the AlN substrate. The grain boundaries are imparted by dispersion strengthening mechanism and in turn improves the microhardness and bending strength.

Hydrogen can facilitate the detachment of protective oxide layer from the metals and alloys. The degradation is usually accelerated at elevated temperatures in many industrial applications [11].

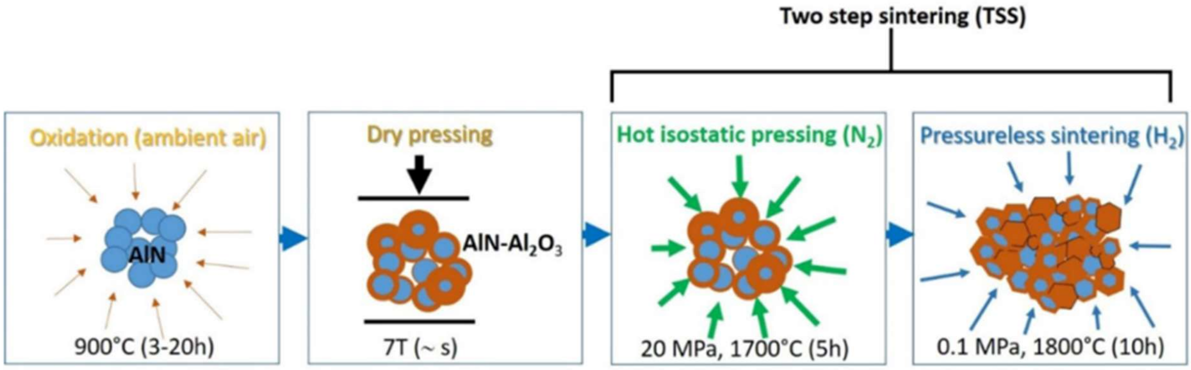

Fig. 6 Experimental procedure of Al_2O_3 sintered sample preparation from AlN powder.

Li et al. studied the effect of hydrogen on the integrity of aluminum–oxide interface at elevated temperatures [11]. Anya et al. used the pressureless sintering (PS) in hydrogen to obtain Al_2O_3-SiC composites [12]. They reported exploration of the effects of sintering variables on the final density and resultant Young's modulus of composites. Taun et al. prepared the Al_2O_3-Ni composites by pressureless sintering in H2 [13]. The sintering had certain effects on mechanical properties of the composites. The toughness of the composites is enhanced by a crack bridging mechanism or by microcrack toughening. However, the strength of the composites is decreased significantly as the microcracks are formed [13].

Our previous study of the structural and mechanical characterizations of HIP sintered AlN-Al_2O_3 was discussed in [14]. A combination of HIP and PS post-sintering was proposed in this work to obtain high-density bodies with higher hardness. In this work, the effect of pressureless sintering in hydrogen on hot isostatic pressed AlN-Al_2O_3 prepared from oxidized AlN powder was studied.

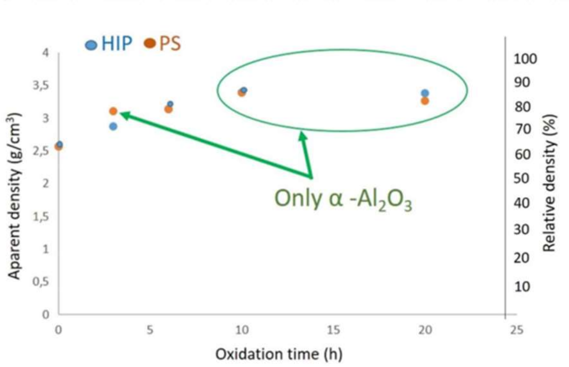

Fig. 7. Apparent and relative density measurements of the HIP and PS samples.

The apparent density measurement can help in the valuable information to control the quality of a ceramic with respect to the porosity. The apparent densities of sintered samples (HIP, PS) are shown in Fig. 7. The comparative study of densities of HIP sintered and PS sintered samples showed the similar tendency. The HIP and PS sintered base (reference) AlN exhibited the lowest apparent density (2.57 g/cm3 , Fig. 7). Increasing of the oxidation time of base AlN powder caused the increasing of density values from 2.87 to 3.38 g/cm3 for HIP (20 hours oxidized powder) and from 3.11 to 3.27 g/cm3 for PS (20 hours oxidized powder), respectively. Kim et al. developed the Al_2O_3 with additions of 1–25 mol% AlN by the reaction sintering in nitrogen gas at 1600–1800 °C, 20 MPa for 2 hours [15]. Sintered Al_2O_3 with 1 mol% AlN addition at 1750 °C resulted close to theoretical density of α-Al_2O_3 (3.98 g/cm3). They observed for the different compositions of AlN-Al_2O_3 that the sintered densities decreased with increasing AlN content [15]. Apparent density values of HIP and post-sintered Al_2O_3 are in agreement with results of group of Kim et al. [15]. The presence only the major α-Al_2O_3 predicted the higher densification during sintering process (independently on sintering type) (Fig. 7). AlN phase blocked the fully densification and caused the formation of the bigger grains, porosities and impurities in sintered ceramics The highest apparent density 3.39 g/ cm3 (85% relative density) has been observed in a case of sample oxidized for 10 hours.

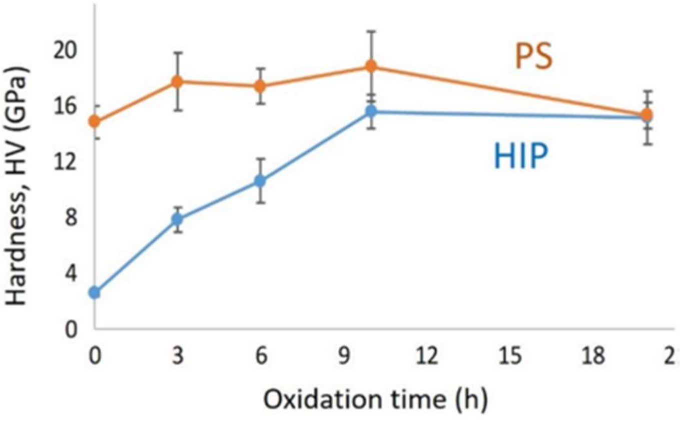

Fig. 8. Hardness of HIP and PS sintered Al_2O_3 versus oxidation time of AlN base powder.

The improvement of the mechanical properties of Al_2O_3 can be expected potential ceramics for novel engine or other applications. Hardness is one of the most important mechanical property. Bocanegra-Bernal et al. obtained hardness of 20.5 ± 0.6 GPa presented a grain size of Al_2O_3 ~ 0.62±0.04 µm at the lowest HIP temperature (1300 °C) [16]. Willmann reported the hardness values of 17–19 GPa for grain size of 4.5, 3.2, and 1.8 µm [17]. Xue et al. applied the hot pressing at various temperatures of 1800, 1850, and 1900 °C and produced the AlN- Al_2O_3 with hardness between 14 and 16 GPa [18]. Hardness values have been characterized as function of oxidation time (Fig. 8). The similar tendency of hardness behavior has been observed for both sintering techniques. The increasing of hardness has been infuenced by increasing of oxidization time of base AlN powder, minimal presence of AlN and grain size of α- Al_2O_3. In addition, reduction of porosity resulted in closer packing, denser structure and improvement the hardness of sintered samples. The highest hardness values between 17 and 18 GPa have been observed for PS sintered α- Al_2O_3 oxidized between 3 and 10 hours. These values are comparable with results of other research groups [16-18].

As a conclusion the following statements can be withdrawn from the study above:

-The preparation of composite AlN- Al_2O_3 ceramics was carried out by oxidation of pure AlN powders and subsequent hot isostatic pressing/pressureless sintering.
-The oxidized AlN powders have developed two distinct phases of aluminum oxide (α- Al_2O_3 and θ- Al_2O_3). The transformation depended on the time of oxidation with lower percentage of conversion obtained after 3 hours and near complete transformation of AlN to Al_2O_3 at 20 hours oxidation.
-The sintered samples showed the presence of only α- Al_2O_3 besides AlN proving that the sintering results in disintegration of θ- Al_2O_3 phase.
-Upon sintering, the substrates showed marked improvement in the density with a reduction in the porosity. The experiments also proved that densification in sintered samples can be achieved by HIP sintering particularly at lower temperatures (< 1800° C). The measured density values were in agreement with values reported in literature.
-Mechanical tests showed considerable improvement in the bending strength and microhardness of the sintered substrates. However, superior properties in both the cases were observed in samples made from 10 hours oxidised powders followed by samples from 20 hours oxidised powders.
-According to the tribology tests, the samples showed considerably good wear property. Furthermore, the extensive tribofilm formation, brittleness and surface cracks observed during the experimentation are due to the presence of clusters of Al_2O_3 at the AlN surface. The extensive tribofilm formation provided a stable friction behavior, whereas the lower amount of tribofilm or no tribofilm formation on smooth surface resulted in unstable frictional behavior.
-The HIP followed by post-sintering of oxidized AlN powder without sintering additives has been successfully developed for the frst time. Post-sintering in 1800 °C for 10 hours caused the phase transformation to α- Al_2O_3 which had efect on the apparent density and hardness of post-sintering sintered ceramics. Te highest apparent densities 3.11–3.39 g/cm3 (78–85% relative densities) and highest hardness values (17–18 GPa) have been measured for post-sintered α- Al_2O_3 prepared from base powder oxidized between 3 and 10 hours.

References

1. McCauley, J.W.; Patel, P.; Chen, M.; Gilde, G.; Strassburger, E.; Paliwal, B.; Dandekar, D.P. AlON: A brief history of its emergence and evolution. J. Eur. Ceram. Soc. 2009, 29, 223–236.
2. Suryanarayana, D. Oxidation kinetics of aluminum nitride. J. Am. Ceram. Soc. 1990, 73, 1108–1110.
3. Bellosi, A.; Landi, E.; Tampieri, A. Oxidation behavior of aluminum nitride. J. Mater. Res. 1993, 8, 565–572.
4. Brown, A.L.; Norton, M.G. Oxidation kinetics of AlN powder. J. Mater. Sci. Lett. 1998, 17, 1519–1522.

5. Lin, C.Y.; Lu, F.H. Oxidation behavior of AlN films at high temperature under controlled atmosphere. J. Eur. Ceram. Soc. 2008, 28, 691–698.
6. Duchesne, D.J.; Hipps, K.W.; Grasher, B.A.; Norton, M.G. The formation of transition aluminas during oxidation of AlN. J. Mater. Sci. Lett. 1999, 18, 877–879.
7. Gu, Z.; Edgar, J.H.; Wang, C.; Coffey, D.W. Thermal oxidation of aluminum nitride powder. J. Am. Ceram. Soc. 2006, 89, 2167–2171.
8. Swab, J.J.; Pavlacka, R.; Gilde, G.; Kilczewski, S.; Wright, J.; Harris, D. Determining the strength of coarse-grained AlON and spinel. J. Am. Ceram. Soc. 2014, 97, 592–600.
9. Quinn, G.D.; Corbin, N.D.; McCauley, J.W. Thermomechanical properties of aluminum oxynitride spinel. Am. Ceram. Soc. Bull. 1984, 63, 723–730.
10. Willems, H.X.; Van Hal, P.F.; Metselaar, R. Mechanical properties of γ-aluminium oxynitride. J. Mater. Sci. 1993, 28, 6185–6189.
11. Li, M. et al. Efect of hydrogen on the integrity of aluminium–oxide interface at elevated temperatures. Nat. Commun. 8 (2017) 14564.
12. Anya, C. C. & Roberts, S. G. Pressureless sintering and elastic constants of A10-SIC nanocomposites. J. Eur. Ceram. Soc. 17, 565–573. (1997).
13. Tuan, W. H., Lin, M. C. & Wu, H. H. Preparation of Al2O3Ni composites by pressureless sintering in H2. Ceram. Int. 21(4), 221–225. (1995).
14. Varanasi, D., Furkó, M., Balázsi, K. & Balázsi, C. Processing of Al_2O_3-AlN ceramics and their structural, mechanical, and tribological characterization. Materials 14(20), 6055 (2021).
15. Y.W. Kim, H.C. Park, Y.B. Lee, K.D. Oh, Stevens, R. Reaction sintering and microstructural development in the system Al_2O_3–AlN, J. Eur. Ceram. Soc. 21(2001) 2383–2391.
16. Bocanegra-Bernal, M. H. et al. Hot isostatic pressing (HIP) of a-Al_2O_3 submicron ceramics pressureless sintered at diferent temperatures: Improvement in mechanical properties for use in total hip arthroplasty (THA). Int. J Refract. Met. Hard Mater. 27, 900–906. (2009).
17. Willmann, G. Ceramic femoral head retrieval data. Clin. Orthop. Relat. Res. 379, 22–28 (2000).
18. Xue, J. M. et al. Hot-pressed translucent aluminum oxynitride (AlON) ceramics. Key Eng. Mater. 368–372, 450–452. (2008).
19. K. Balázsi, D.Varanasi, Zs. E. Horváth, M. Furkó, F. S. Cinar & C. Balázsi, Efect of the pressureless post-sintering on the hot isostatic pressed Al_2O_3 prepared from the oxidized AlN powder, Scientifc Reports, (2022) 12:8250.